International Journal of Engineering Inventions
e-ISSN: 2278-7461, p-ISSN: 2319-6491
Volume 13, Issue 8 [August. 2024] PP: 66-74

Design and Mechanical Performance Analysis of Lower Extremity Exoskeleton Devices

Chunshan He, Xiaoying Ma, Shixin Dou, Liai Pan, Zhenhua Hou
Shool of Mechanical and Vehicle Engineering, Changchun University, Changchun, CHINA
Corresponding Author: Zhenhua Hou .

ABSTRACT: *In response to the current aging of China's population and the increasing demand for rehabilitation-assisted exoskeletons, a steerable lower limb exoskeleton device is designed with reference to ergonomic standards, which can be more efficient when encountering the need to change the direction of walking, and provides diversified movement modes to the user. In this paper, we use SolidWorks for the construction of 3D model and detailed design for hip and leg. After simplifying the structure, ANSYS was used to analyze the stress and strain of the exoskeleton in two-legged standing and one-legged standing, and then the modal analysis was used to solve the first 10 orders of vibration pattern to get the intrinsic frequency of the exoskeleton to make sure that no resonance would occur when wearing and using. And the results proved that the selected materials and the designed structure meet the requirements.*
Keywords: *Lower limb rehabilitation, Exoskeletal structure, Static analysis, Modal analysis*

Date of Submission: 05-08-2024 Date of acceptance: 16-08-2024

I. INTRODUCTION

In recent years, the aging problem in China has been increasing, and the age structure of the population is undergoing a radical change, the aging of the population in China has become a problem that cannot be ignored [1-2]. China is accelerating into aging and the market demand for exoskeletons with rehabilitation assistance is increasing [3]. The widespread use of rehabilitation exoskeletons is gradually changing the role of the medical professional as a powerful aid in assisting patients with prolonged and repetitive rehabilitation [4]. Lower limb exoskeleton devices are devices worn on the human lower limbs and controlled to accomplish specific movements to provide continuous, effective, and multimodal rehabilitation for patients with their unique features [5]. It not only enhances the patients' awareness to actively participate in the training, but also significantly accelerates the recovery process of the patients' lower limb motor function and helps them to realize normal walking. By applying rehabilitation exoskeletons, patients can return to normal life faster and better and enjoy a higher quality of life [6]. Therefore, the exoskeleton for lower limb rehabilitation has a wide range of research and application value, and has a broad development prospect in the future. Both domestic and foreign countries are increasing the research on the exoskeleton.

Chang et al [7] designed a lower limb rehabilitation exoskeleton robot driven by disk motors and showed experimentally that both its passive and resistance rehabilitation training modes help to rehabilitate the lower limbs of hemiplegic patients. Wei et al [8] designed a multi-degree-of-freedom adjustable lower limb rehabilitation exoskeleton using a screw mechanism with added rotational degrees of freedom at the waist. Qiu et al [9] designed a passive ankle-assisted exoskeleton by utilizing the principle of a clutch and spring in conjunction with a booster leg. A research and development team at Vanderbilt University (Vanderbilt) has developed an exoskeleton device called Indego that works in much the same way that humans learn to walk [10]. The Hybrid Assistive Limb (HAL), developed in Japan in collaboration with the University of Tsukuba and Cyberdyne, can provide real-time on-demand assistance to patients to extend their walking time [11].

Currently, exoskeleton devices used for patients in China are assisting straight-line walking and lack functions such as leg bending, lifting and dropping, steering, and assisted support in height direction. For cases where the walking direction needs to be changed, the patient usually needs to stop and readjust, requiring the help of a family member or caregiver, resulting in more time and physical effort in actual use.So making it difficult to achieve coordinated coordination of the various mechanisms during auxiliary movements in the steering maneuver. The above problems need to be solved urgently as the single training mode is unable to provide diversified exercise patterns, which is not conducive to the effectiveness of rehabilitation training.

Therefore, this paper innovates the body structure of the lower limb rehabilitation exoskeleton, designs a lower limb exoskeleton that can realize steering, and verifies the reasonableness of the design through static and modal analysis, which can provide users with diversified training modes.

II. Lower Extremity Rehabilitation Exoskeleton Device Design

After formulating the design scheme, the dimensions of each component of the lower limb rehabilitation exoskeleton device are designed using SolidWorks 3D modeling software. The overall structure of the lower limb exoskeleton device is illustrated in Figure 1, with detailed design specifications as follows.

(1) Referring to the anthropometric basic data in the GB 1000-1988 standard and adjusting it appropriately in combination with the actual situation, the lower limb exoskeleton mechanism is designed to have a thigh length of 430 mm, a calf length of 400 mm, a waist circumference of 720 mm and a foot length of 260 mm.

(2) The device mainly includes straps, hip joint steering mechanism, thigh mechanism, calf mechanism, and foot assembly. The device is driven by a servo motor. In order to ensure real-time interaction between the lower limb rehabilitation exoskeleton and the human leg, a binding device is installed on the calf adjustment lever to tightly connect the exoskeleton with the human leg through a strap.

Fig. 1 Schematic diagram of the overall structure of the lower limb exoskeleton device

2.1 Exoskeleton hip design

According to the principle of human anatomy, the hip joint of the human body is a ball-and-socket structure with a fixed center of rotation and three degrees of freedom. However, if the ball-and-socket structure is directly used in design, although it can meet the requirements to the greatest extent, it requires too much control and drive [12-13]. Therefore, the hip joint designed in this article is shown in Figure 2, with its steering set at the waist and connected to the waist mechanism to reduce the error of joint movement. There is a motor drive system at the hip joint, which is transmitted through a gear mechanism, and the output shaft is driven by a shaft key to rotate the steering plate.

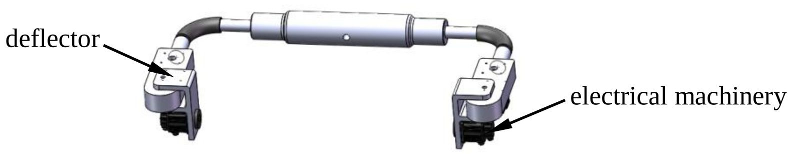

Fig. 2 Schematic diagram of lower extremity exoskeleton hip joints

2.2 Exoskeleton leg design

The leg structure of the lower limb rehabilitation exoskeleton designed in this paper primarily comprises a knee joint drive unit, a thigh connecting rod, and a calf adjustment rod, as illustrated in Figure 3. During daily walking, the knee joint primarily undergoes flexion and extension movements, thus it can be considered as a single-degree-of-freedom hinge joint. The rod surface features positioning holes every 10mm, allowing for sizing adjustments to cater to various users. Additionally, given the curvature of the human leg, the rods are curved to enhance the wearing comfort of the users.

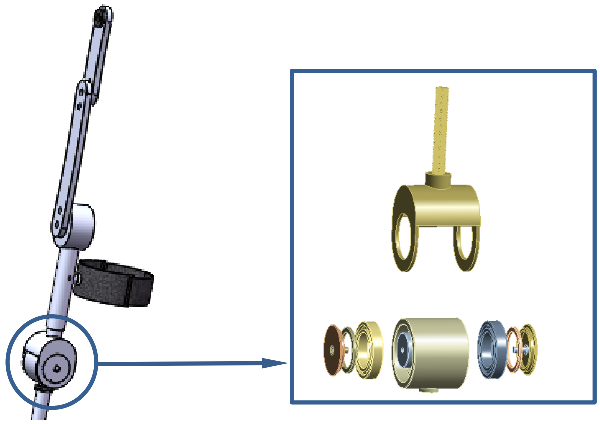

Fig. 3 Schematic representation of the lower extremity exoskeleton leg and adjusting screw sleeve

III. Static analysis of exoskeleton device based on ANSYS

3.1 Fundamentals of Linear Static Analysis

From the theory of classical mechanics, the generalized equation for the dynamics of an object is

$$\boldsymbol{M}\boldsymbol{x}'' + \boldsymbol{C}\boldsymbol{x}' + \boldsymbol{K}\boldsymbol{x} = \boldsymbol{F}(\boldsymbol{t}) \quad (1)$$

In the equation, $\boldsymbol{M}$ denotes the mass matrix, $\boldsymbol{C}$ denotes the damping matrix, $\boldsymbol{K}$ denotes the stiffness matrix, $\boldsymbol{x}$ represents the displacement vector, $\boldsymbol{F(t)}$ stands for force, $\boldsymbol{x}'$ represents the velocity vector, and $\boldsymbol{x}$ signifies the acceleration vector.

In the current structural analysis, the quantities related to time t are ignored, and so equation (1) can be simplified to:

$$\boldsymbol{K}\boldsymbol{x} = \boldsymbol{F} \quad (2)$$

3.2 Static modeling

The basic requirement for the lower limb exoskeleton is to ensure the safety of the wearer. Therefore, the static strength of the structure under given boundary conditions can be directly obtained by using the finite element method for static analysis. In this way, the stress and strain of the lower limb exoskeleton can be obtained, and then the strength and stiffness of the overall structure can be verified.

3.3 Finite element modeling of the exoskeleton

Before using Workbench for the hydrostatic analysis of the lower limb exoskeleton, the most important work is the geometric modeling, this is because the good or bad geometric modeling will directly affect the correctness of the calculation results. Generally, the geometric modeling work occupies a very large amount of time and is very important in the whole finite element analysis process.

Initially, the model of the exoskeleton in various states is simplified in SolidWorks. Since this is a static analysis, the flexible binding structure, which has no practical effect, can be directly removed and saved in STP format before being imported into ANSYS Workbench.

3.4 Delineation of the grid

The types of element bodies include tetrahedral mesh, hexahedral mesh, automatic mesh generation, etc. Because tetrahedral element is suitable for different structures, it can simulate any shape in three-dimensional space, and has good mathematical stability. Even under very large deformation, it is not easy to produce calculation error, and has high calculation accuracy. Therefore, tetrahedral elements are selected to divide the mesh in this paper. The total number of grids is 323087 and the total number of nodes is 600127. As shown in Figure 4:

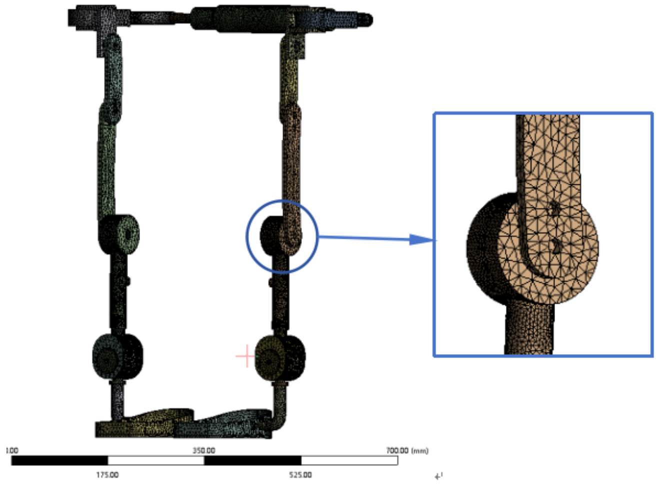

Fig. 4 Lower extremity exoskeleton tetrahedral meshing diagram

3.5 Selection of materials

The material of the main part of the exoskeleton device is aluminum alloy 7075, which has high hardness, high strength, good welding performance and corrosion resistance, with a modulus of elasticity of 71 Gpa and a yield strength of 455 MPa. At the same time, nylon was chosen as the material of the strap to prevent the strap from slipping and stretching, and its width was set at 130 mm.

3.6 Defining loads

For the exoskeleton, the load is mainly the lower limb exoskeleton and the user's own weight. Since the human body is in circular motion when walking, the force applied to the lower limb exoskeleton is different under different gaits. Therefore, the sum of the weight of the human machine is determined to be 1200 N after comprehensive consideration, and different loads and constraints are applied to the exoskeleton when standing on two legs and one leg respectively. In this paper, the static analysis of the standing phase supported by legs was carried out by setting the fixed constraint on both feet and applying a vertical downward load of 1200 N on both sides of the hip joint. This is because the lower limb exoskeleton fully carried the man-machine weight when it was in the standing phase, as shown in Figure 5 (a). In the statics analysis of the standing phase of single-leg support, the left supporting leg should bear the maximum load, and the right supporting leg should also be strongly balanced. Therefore, 900 N vertical downward load is applied to the left side of the hip joint of the exoskeleton, and 300 N vertical downward load is applied to the right side of the hip joint, as shown in Figure 5 (b).

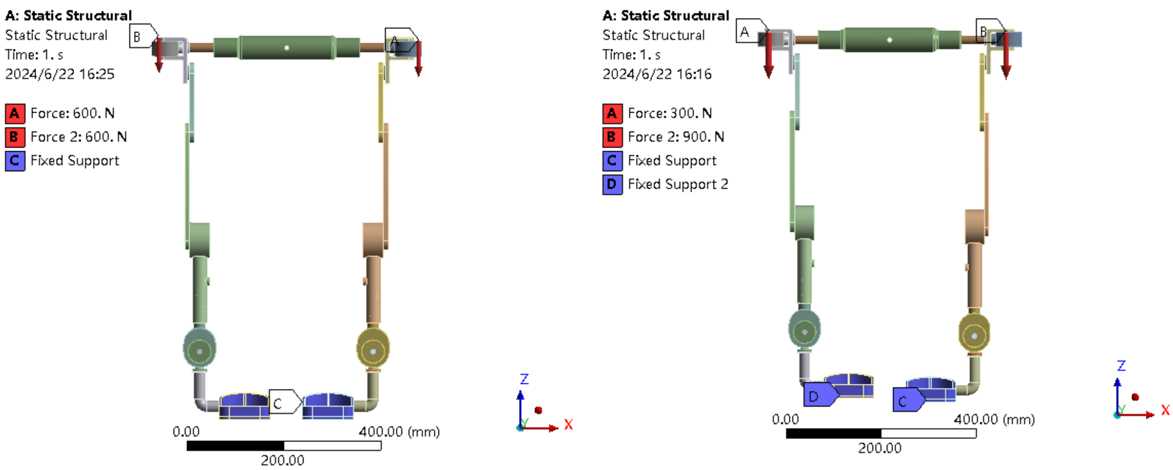

(a) double support phase (b) Single leg support phase

Fig. 5 Schematic illustration of constraints and loads in a lower extremity exoskeleton

3.7 Static analysis results

The finite element model of lower limb exoskeleton was established based on Workbench and statics analysis was carried out. The total deformation analysis cloud image of exoskeleton under the above two different gaits was obtained in the Workbench post-processing module, as shown in Figure 6:

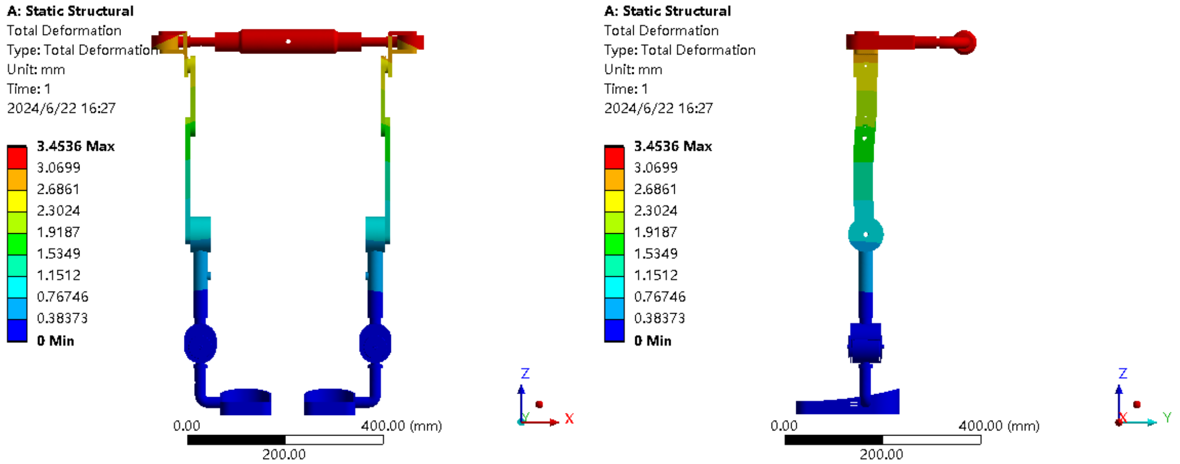

(a) double support phase

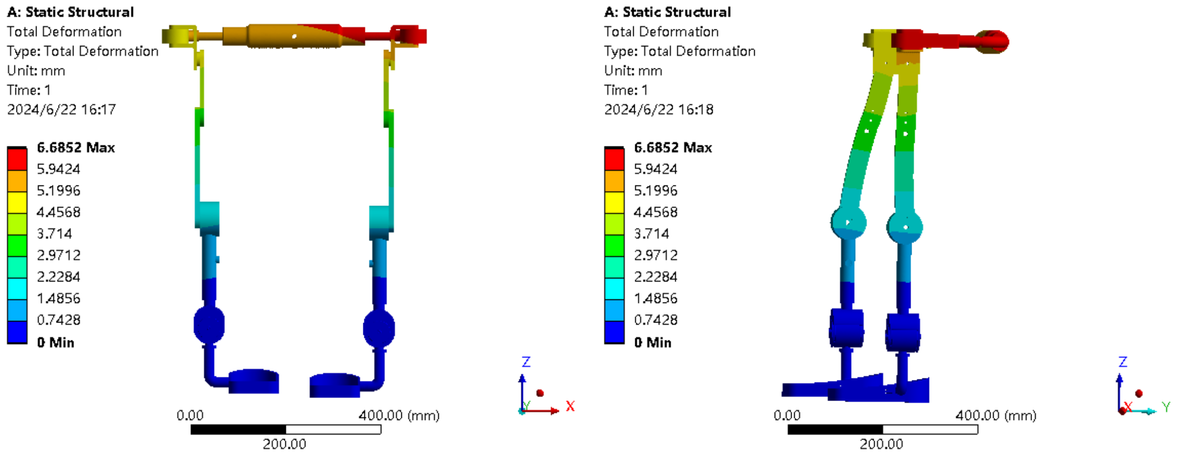

(b) Single leg support phase

Fig. 6 Cloud view of total deformation analysis of lower extremity exoskeleton

The deformation of the exoskeleton under the support phase of both legs is shown in Figure 6 (a). The maximum deformation is located at the bracket and hip joint, which is 3.453 mm, the deformation displacement of the knee joint is 0.767 mm, and the deformation displacement of the ankle joint is 0.383 mm. The overall displacement deformation trend shows that it decreases from top to bottom. The deformation of the exoskeleton under the single leg support phase is shown in Figure 6 (b). Because it is mainly supported by the left side of the exoskeleton, the maximum deformation occurs at the left bracket and hip joint of the exoskeleton, which is 6.685 mm, the deformation displacement of the knee joint is 1.485 mm, and the deformation displacement of the ankle joint is 0.742 mm.

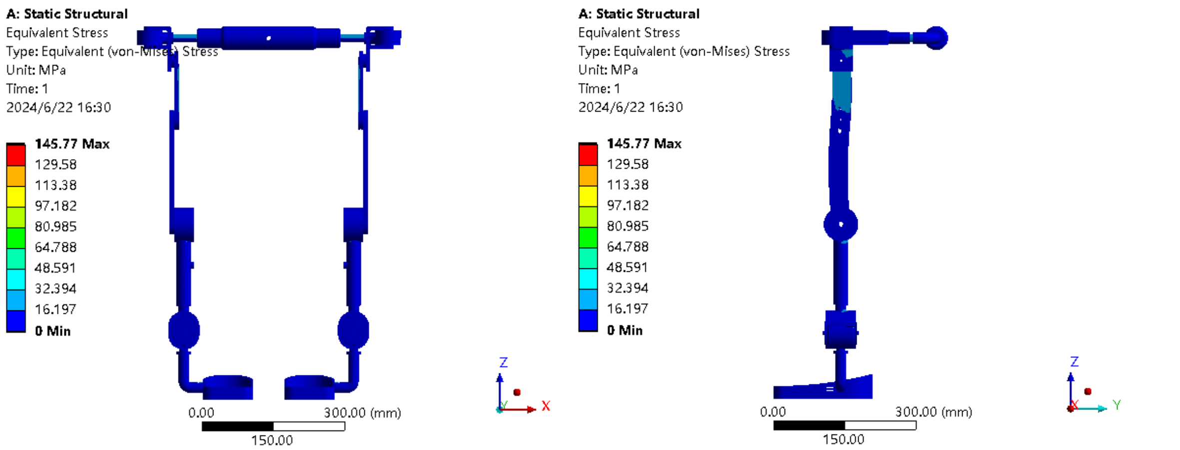

(a)double support phase

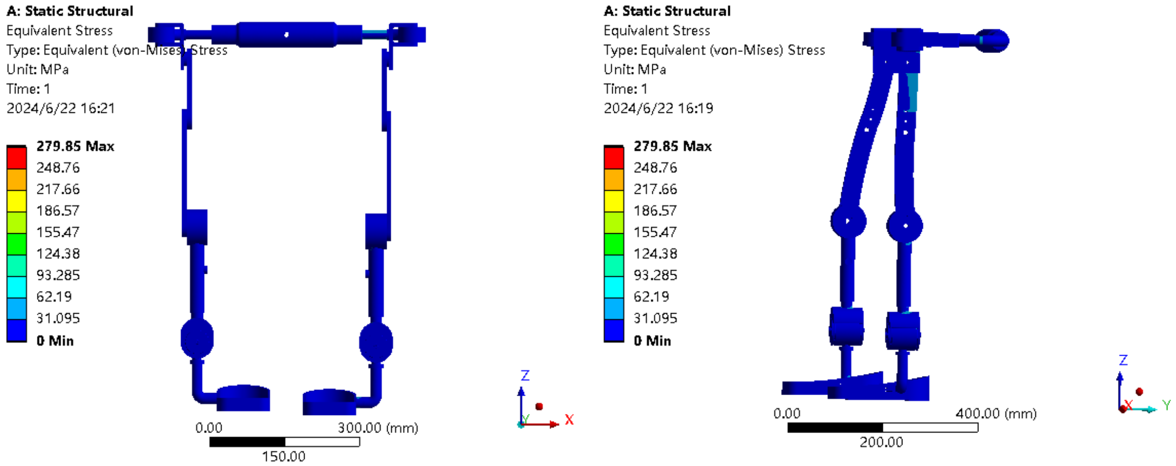

(b)Single leg support phase

Fig. 7 Lower extremity exoskeleton stress analysis cloud map

The stress nephogram of the lower limb exoskeleton under two different gaits is shown in Figure 7. The stress of the leg support phase is shown in Figure 7 (a). The maximum stress is located in the center of the support, which is 145.77 MPa. The stress of single leg support phase is shown in Figure 7 (b), and the maximum stress is 279.85 MPa. According to the stress distribution of the two gait patterns, it can be seen that the yield strength of the selected material is 455 MPa smaller than that of aluminum alloy 7075, and its maximum stress and deformation are within the allowable range, indicating that the properties of the selected material meet the design requirements.

IV. Modal Analysis

When the human body wears the exoskeleton robot for walking, the exoskeleton robot will receive the impact and vibration from the ground, and will also be affected by the vibration between the motor and reducer. These vibrations will also affect the structure of the whole machine to produce corresponding vibration. If the natural vibration frequency is the same as the motor frequency, it may cause resonance, which will not only lead to the deformation of the robot structure, but also affect the accuracy of the control system and the sensing system. Therefore, the modal analysis of the exoskeleton robot is required [14-15].

4.1 Fundamentals of Modal Analysis

The undamped modal analysis is a classical eigenvalue problem, and the kinematic equation of the dynamic problem is

$$\boldsymbol{M}\boldsymbol{x}'' + \boldsymbol{K}\boldsymbol{x} = 0 \quad (3)$$

The free vibration of the structure is simple harmonic vibration, that is, the displacement is a sine function:

$$\boldsymbol{x} = \boldsymbol{x}\sin(\omega t) \quad (4)$$

Substituting in formula (3) yields:

$$\left(\boldsymbol{K} - \omega^2 \boldsymbol{M}\right)\boldsymbol{x} = \{0\} \quad (5)$$

Equation (3) is a classical eigenvalue problem, the eigenvalue of this equation is ω_i^2, and its square root ω_i is the natural vibration circular frequency, the natural vibration frequency is $f = \frac{\omega_i}{2\pi}$.

The eigenvector $\boldsymbol{x}_i$ corresponding to the eigenvalue ω_i^2 is the vibration mode corresponding to the self-oscillation frequency $f = \frac{\omega_i}{2\pi}$.

4.2 Modal analysis results

Modal analysis can not only help determine the natural frequency and mode of the structure, so that the designed structure can avoid resonance, but also estimate the control parameters in the dynamic analysis. The first 10 frequencies and vibration modes of the modal analysis of the lower limb exoskeleton device are shown in Figure 8:

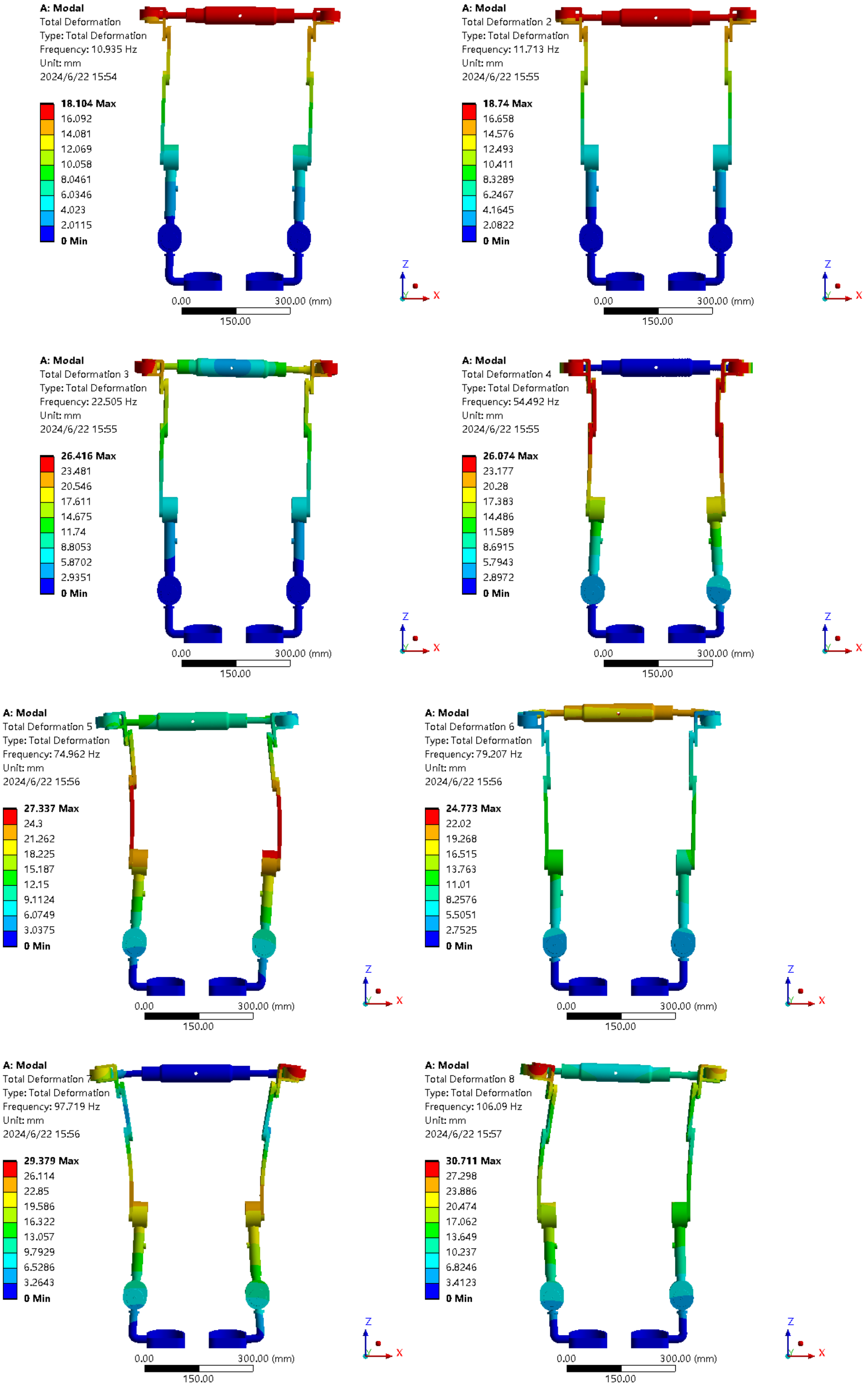
A: Modal
Total Deformation
Type: Total Deformation
Frequency: 10.935 Hz
Unit: mm
2024/6/22 15:54
18.104 Max
16.092
14.081
12.069
10.058
8.0461
6.0346
4.023
2.0115
0 Min
0.00
300.00 (mm)
150.00
A: Modal
Total Deformation 2
Type: Total Deformation
Frequency: 11.713 Hz
Unit: mm
2024/6/22 15:55
18.74 Max
16.658
14.576
12.493
10.411
8.3289
6.2467
4.1645
2.0822
0 Min
0.00
300.00 (mm)
150.00
A: Modal
Total Deformation 3
Type: Total Deformation
Frequency: 22.505 Hz
Unit: mm
2024/6/22 15:55
26.416 Max
23.481
20.546
17.611
14.675
11.74
8.8053
5.8702
2.9351
0 Min
0.00
300.00 (mm)
150.00
A: Modal
Total Deformation 4
Type: Total Deformation
Frequency: 54.492 Hz
Unit: mm
2024/6/22 15:55
26.074 Max
23.177
20.28
17.383
14.486
11.589
8.6915
5.7943
2.8972
0 Min
0.00
300.00 (mm)
150.00
A: Modal
Total Deformation 5
Type: Total Deformation
Frequency: 74.962 Hz
Unit: mm
2024/6/22 15:56
27.337 Max
24.3
21.262
18.225
15.187
12.15
9.1124
6.0749
3.0375
0 Min
0.00
300.00 (mm)
150.00
A: Modal
Total Deformation 6
Type: Total Deformation
Frequency: 79.207 Hz
Unit: mm
2024/6/22 15:56
24.773 Max
22.02
19.268
16.515
13.763
11.01
8.2576
5.5051
2.7525
0 Min
0.00
300.00 (mm)
150.00
A: Modal
Total Deformation 7
Type: Total Deformation
Frequency: 97.719 Hz
Unit: mm
2024/6/22 15:56
29.379 Max
26.114
22.85
19.586
16.322
13.057
9.7929
6.5286
3.2643
0 Min
0.00
300.00 (mm)
150.00
A: Modal
Total Deformation 8
Type: Total Deformation
Frequency: 106.09 Hz
Unit: mm
2024/6/22 15:57
30.711 Max
27.298
23.886
20.474
17.062
13.649
10.237
6.8246
3.4123
0 Min
0.00
300.00 (mm)
150.00

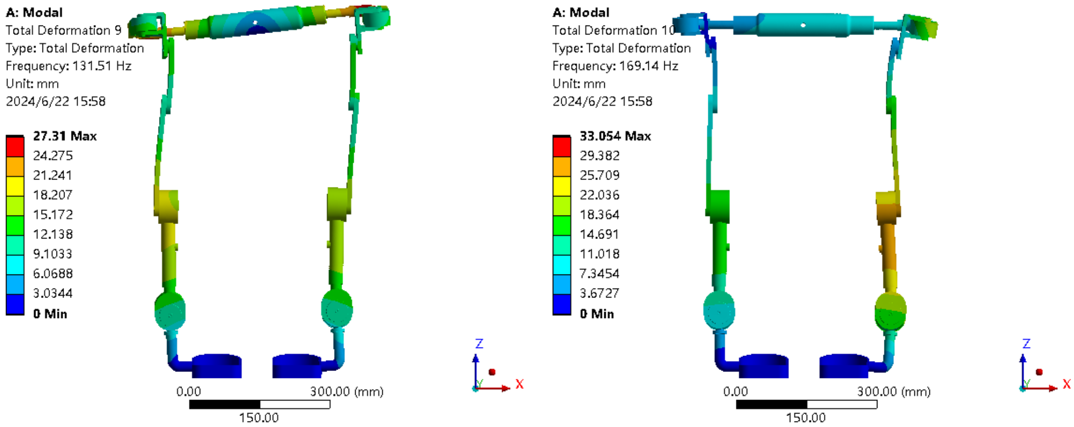

Fig. 8 Results of the 10th order modal analysis of the lower limb exoskeleton

Table 1 First 10 orders of intrinsic frequency in lower limb exoskeletons

Modal order	Natural frequency/Hz
1	10.935
2	11.713
3	22.505
4	54.492
5	74.962
6	79.207
7	97.719
8	106.19
9	131.51
10	169.14

In a study of human walking movement patterns, it was found that the human body oscillates at a frequency of 2 Hz during walking and 4 Hz during running [16]. The natural frequencies of lower limb exoskeleton obtained from modal analysis in this section are shown in Table 1. It can be seen that they are quite different from these two swinging frequencies, so the wearer and exoskeleton robot will not resonate during normal walking.

V. Summary

This study employs SolidWorks to design a three-dimensional model for the lower limb exoskeleton device. One motor controls the rotation of the exoskeleton's hip joint, while another motor manages the swing of the thigh link, which in turn elevates and lowers the entire mechanical skeleton. The knee joint also incorporates a motor, enabling controlled and coordinated movement for walking, significantly enhancing the user's range of motion. For individuals requiring rehabilitation training, this device offers a variety of motion patterns, facilitating muscle recovery. Following structural design, the device underwent finite element analysis using ANSYS, including static and modal analyses. The static analysis revealed that during the bipedal support phase, the exoskeleton experienced a maximum strain of 3.453 mm and a maximum stress of 145.77 MPa. During the unipedal support phase, the maximum strain reached 6.685 mm and the maximum stress 279.85 MPa, all within acceptable limits. Modal analysis further determined the natural frequencies of each mode, preventing resonance during structural movement.

REFRENCES

[1]. Zhang X Y. Research on the current characteristics, development trend and countermeasures of population aging in China [J]. China Management Information Technology, 2019,23(05):195-199.

[2]. Liu X, Zhu J, Zou K. The development trend of China's aging population: a forecast perspective[J]. Complex & Intelligent Systems, 2022, 8(4): 3463-3478.

[3]. Kapsalyamov A, Jamwal P K, Hussain S, et al. State of the art lower limb robotic exoskeletons for elderly assistance[J]. IEEE Access, 2019, 7: 95075-95086.

[4]. CHENG Xue,BAI Dingqun,PENG Xiaohua. Application and research progress of lower limb exoskeleton rehabilitation robot in stroke rehabilitation[J]. Chinese Journal of Rehabilitation Medicine,2021,36(10):1327-1332.

[5]. BAI Xue,LIANG Wenyuan,WANG Qiang,et al. Research progress and trend of lower limb exoskeleton robot[J]. China Science and Technology Information,2023,(17):146-149.

[6]. Gao M, Wang Z, Li S, et al. Design and optimization of exoskeleton structure of lower limb knee joint based on cross four-bar linkage[J]. AIP Advances, 2021, 11(6).
[7]. CHANG Jiachen,HAN Yali,SUN Han,et al. Design and performance analysis of exoskeleton robot for lower limb rehabilitation[J]. Journal of Engineering Design,2024,31(02):210-220.
[8]. WEI Xiaoxiao,BI Wenlong,LI Yanan,et al. Design and simulation of a multi-degree-of-freedom adjustable lower limb rehabilitation exoskeleton[J]. Mechanical Transmission,2024,48(01):61-66.
[9]. QIU Zhiyu,ZHU Songqing,HAN Yali,et al. Design and simulation of passive ankle-assisted exoskeleton mechanism[J/OL]. Mechanical Science and Technology:1-9[2024-05-25].
[10]. Tefertiller C, Hays K, Jones J, et al. Initial outcomes from a multicenter study utilizing the indego powered exoskeleton in spinal cord injury[J]. Topics in spinal cord injury rehabilitation, 2018, 24(1): 78-85.
[11]. LIU Ruiping,OU Yangjun. Development and application of lower limb exoskeleton rehabilitation robot[J]. Journal of Sun Yat-sen University (Medical Science Edition),2023,44(02):354-360.
[12]. XI Peng-Yu,ZHANG Zhi-Li,ZIELINSKA Teresa,et al. Design and finite element analysis of a lower limb exoskeleton robot[J]. Journal of Tianjin Polytechnic University,2022,38(01):1-7.
[13]. DU DINGYAO. Structural design and simulation of key components for exoskeleton robots[J]. Engineering Machinery, 2020, 51(10): 81-87.
[14]. ZHU Yaqiao, ZHANG Jianhua, WANG Jiaojiao, et al. Modal and fatigue analysis of a finite element-based assisted exoskeleton robot[J]. Science, Technology and Engineering, 2020, 20(1) : 6916-6922.
[15]. YANG Fan, XIE Rukun, LIU Fanghua. Structural design and simulation analysis of lower limb exoskeleton [J]. Machinery and Electronics, 2019, 37(2): 198-204.
[16]. Wang Fangzheng. Structural design and simulation analysis of single lower limb exoskeleton robot [D]. Beijing: Beijing Forestry University, 2017.